AIAA JOURNAL
Vol. 44, No. 5, May 2006

Technical Notes

TECHNICAL NOTES are short manuscripts describing new developments or important results of a preliminary nature. These Notes should not exceed 2500 words (where a figure or table counts as 200 words). Following informal review by the Editors, they may be published within a few months of the date of receipt. Style requirements are the same as for regular contributions (see inside back cover).

Efficient Shape Optimization Under Uncertainty Using Polynomial Chaos Expansions and Local Sensitivities

Nam H. Kim,* Haoyu Wang,† and Nestor V. Queipo‡
University of Florida, Gainesville, Florida 32606

I. Introduction

RELIABILITY-BASED design optimization (RBDO) involving a computationally demanding model has been limited by the relatively high number of required analyses for uncertainty propagation during the design process. To overcome this limitation, several alternatives, such as moment-based methods[1–4] and the stochastic response surface approach,[5–8] have been proposed. The moment based-methods are relatively efficient because they approximate the performance measure at the most probable point. However, the accuracy of these approximations is a concern when the function exhibits nonlinear behavior.

The stochastic response surface (SRS) approach models the performance function as the sum of elementary functions (bases) of stochastic input parameters and is particularly useful in computationally intensive applications. However, this approach leaves open two issues that critically affect its effectiveness/efficiency: the nature of the elementary functions and the number and location of the sampling points.

This Note presents an efficient shape optimization technique that addresses the referenced issues based on SRS constructed using outputs at heuristically selected collocation points. The proposed SRS is a polynomial chaos expansion that uses Hermite polynomial bases and provides a closed-form approximation of outputs from a significant lower number of model simulations than those required by conventional methods. The efficiency and convergence of the proposed approach are demonstrated using an industrial design problem.

II. Uncertainty Propagation and Polynomial Chaos Expansions

Uncertainty quantification can be decomposed in three fundamental steps: 1) uncertainty characterization of inputs, 2) propagation of uncertainty, and 3) uncertainty management. The uncertainties in inputs are represented in terms of standard normal random variables (SRV). For other types of random variables, either different polynomial bases[9] or appropriate transformation can be used.

The uncertainty propagation is based on constructing SRS (polynomial chaos expansion). The polynomial expansion uses Hermite bases for the space of square-integrable probability density functions (PDF). The SRS has been applied for various applications, including biological systems,[6] tolerance analysis,[7] and electric systems.[8]

Let n be the number of random variables and p the degree of expansion. The output can then be expressed in terms of SRV $\{\xi_i\}$ as

$$y^{(p)} = a_0^{(p)} + \sum_{i=1}^{n} a_i^{(p)}\Gamma_1(\xi_i) + \sum_{i=1}^{n}\sum_{j=1}^{i} a_{ij}^{(p)}\Gamma_2(\xi_i,\xi_j) + \sum_{i=1}^{n}\sum_{j=1}^{i}\sum_{k=1}^{j} a_{ijk}^{(p)}\Gamma_3(\xi_i,\xi_j,\xi_k) + \cdots \quad (1)$$

where the $a_i^{(p)}, a_{ij}^{(p)}, \ldots,$ are deterministic coefficients to be estimated and $\Gamma_m(\xi_1,\ldots,\xi_m)$ are multidimensional Hermite polynomials of degree m given by

$$\Gamma_m(\xi_i,\ldots,\xi_m) = (-1)^m e^{1/2\xi^T\xi}\frac{\partial^m}{\partial\xi_i\ldots\partial\xi_m}e^{-1/2\xi^T\xi} \quad (2)$$

where $\boldsymbol{\xi}$ is the vector of m independent and identically distributed. In general, the approximation accuracy increases with the order of the polynomial, which should be selected reflecting the accuracy needs and computational constraints. The unique feature of the polynomial chaos expansion is that it uses the SRV and Hermite bases. Because of the property that the Hermite bases are orthogonal with respect to an inner product defined using Gaussian measures, the polynomial chaos expansion in Eq. (1) is convergent in the mean-square sense.[9]

The coefficients in the polynomial chaos expansion are calculated as those providing the best fit (least-squares solution) considering a sample of input/output pairs. Because all inputs are represented using SRV, more accurate estimates for the coefficients can be expected if the probability distribution of ξ_i is considered. Hence, a set of points near the high-probability region is heuristically selected among the roots of the one-order higher polynomial under restrictions of symmetry and closeness to the mean.

III. Improving the Efficiency of SRS Using Local Sensitivity Information

In the proposed SRS, the number of sampling points depends on the number of unknown coefficients. Although the proposed method is accurate and robust, we have to address the curse of dimensionality: As the number of random variables increases, the number of coefficients rapidly increases. If local sensitivity information is available, then $n+1$ data at each sampling point can be used for constructing the SRS, which significantly reduces the required number of sampling points. Isukapalli et al.[10] used an automatic differentiation program ADIFOR to calculate the local sensitivity of the output with respect to random variables.

In this Note, continuum-based design sensitivity analysis is utilized to calculate the gradient of the output with respect to random variables. Recent review of the method can be found by Choi and

Received 23 August 2004; revision received 21 September 2005; accepted for publication 13 November 2005.

*Assistant Professor, Department of Mechanical and Aerospace Engineering; nkim@ufl.edu. Member AIAA.
†Graduate Student, Department of Mechanical and Aerospace Engineering. Member AIAA.
‡Visiting Professor, Department of Mechanical and Aerospace Engineering; also Professor, Applied Computing Institute, Faculty of Engineering, University of Zulia, Maracaibo, Venezuela.

Kim.[11] Let z be the displacement and $\bar{z}$ be the displacement variation that belongs to the space $\mathbb{Z}$ of kinematically admissible displacements. For given body force $\boldsymbol{f}$ and surface traction force $\boldsymbol{t}$, the variational equation is formulated as

$$a(z,\bar{z}) := \iint_{\Omega} \sigma_{ij}(z)\varepsilon_{ij}(\bar{z})\,\mathrm{d}\Omega = \iint_{\Omega} f_i\bar{z}_i\,\mathrm{d}\Omega + \int_{\Gamma_T} t_i\bar{z}_i\,\mathrm{d}\Gamma := \ell(\bar{z}) \tag{3}$$

for all $\bar{z} \in \mathbb{Z}$. To solve Eq. (3) numerically, the finite element-based method or the meshfree method can be employed, which ends up solving the matrix equation $[\boldsymbol{K}]\{\boldsymbol{D}\} = \{\boldsymbol{F}\}$.

In design sensitivity analysis, the variational Eq. (3) is differentiated with respect to design variables. Suppose that the initial structural domain Ω is changed into the perturbed domain Ω_τ in which the parameter τ controls the shape perturbation amount. When the design changing direction is defined to be $\boldsymbol{V}(\boldsymbol{x})$, the material point at the perturbed design can be denoted as $\boldsymbol{x}_\tau = \boldsymbol{x} + \tau\boldsymbol{V}(\boldsymbol{x})$. The solution $z_\tau(\boldsymbol{x}_\tau)$ of the structural problem is assumed a differentiable function with respect to shape design. The sensitivity of $z_\tau(\boldsymbol{x}_\tau)$ at $\boldsymbol{x}_\tau$ is defined as

$$\dot{z} = \lim_{\tau\to 0} \frac{z_\tau[\boldsymbol{x} + \tau\boldsymbol{V}(\boldsymbol{x})] - z(\boldsymbol{x})}{\tau} \tag{4}$$

The design sensitivity equation is obtained by taking the material derivative of the variational equation (3). If the applied load is independent of displacement, that is, conservative, then the design sensitivity equation is obtained as

$$a_\Omega(\dot{z},\bar{z}) = \iint_{\Omega} \left[\bar{z}_i \frac{\partial f_i}{\partial x_j} V_j + \bar{z}_i f_i \frac{\partial V_j}{\partial x_j}\right]\mathrm{d}\Omega - \iint_{\Omega} \left[\varepsilon^V_{ij}(\bar{z})\sigma_{ij}(z) + \varepsilon_{ij}(\bar{z})c_{ijkl}\varepsilon^V_{kl}(z) + \varepsilon_{ij}(\bar{z})\sigma_{ij}(z)\,\mathrm{div}\boldsymbol{V}\right]\mathrm{d}\Omega \tag{5}$$

for all $\bar{z} \in \mathbb{Z}$. In Eq. (5),

$$\varepsilon^V_{ij}(z) = -\frac{1}{2}\left(\frac{\partial z_i}{\partial x_k}\frac{\partial V_k}{\partial x_j} + \frac{\partial z_j}{\partial x_k}\frac{\partial V_k}{\partial x_i}\right) \tag{6}$$

Note that by substituting $\dot{z}$ into z the left-hand side of the design sensitivity equation (5) takes the same form as that of the response analysis in Eq. (3). Thus, the same stiffness matrix $[\boldsymbol{K}]$ can be used for sensitivity analysis and response analysis, with a different right-hand side for the fictitious load. Once you calculate the sensitivity $\dot{z}$ of the field vector, the sensitivity of the performance function can be calculated using the chain rule of differentiation.

When finite element analysis is used, the sensitivity equation can be solved inexpensively because the coefficient matrix is already factorized when solving Eq. (3) and the sensitivity equation uses the same coefficient matrix. The computational cost of sensitivity analysis is usually less than 20% of the original analysis cost. The efficiency of the uncertainty propagation approach is critical to RBDO because at each design cycle an updated version of the PDF for the constraint function is required.

IV. Case Study: Torque-Arm Problem

The torque-arm model[12] is used in shape optimization, as shown in Fig. 1. The left hole of the structure is fixed, and an inclined force is applied at the center of the right hole. The meshfree method is employed for the numerical model.[12] The torque-arm is made of steel with stiffness of 207 GPa and Poisson's ratio of 0.3. In Fig. 1, the relative coordinate change of the boundary curve is defined as a random variable and the mean value of random variable is defined as a design parameter.

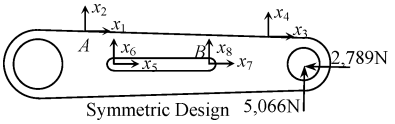

Fig. 1 Torque arm model and random variables.

The design goal is to minimize the mass of the structure by changing the shape of the geometry, which can be modified by moving the boundary curves. The locations of boundary curves are associated with probabilistic distributions due to manufacturing tolerances. The relative locations of corner points of the boundary curves are defined as random variables. For simplicity, we assumed that all random variables exhibit a normal distribution with mean $\mu_i = 0$ and standard deviation $\sigma_i = 0.1$, that is, $\boldsymbol{x} \sim [N(0, 0.1^2)]$. The mean values of these random variables are chosen as design parameters d_i, whereas the standard deviation remains constant during the design process. The initial model consists of eight design parameters.

In the initial design, the maximum stress of 319 MPa occurs at location A in Fig. 1. The stress limit is established to be $\sigma_{\text{limit}} = 800$ MPa. In the reliability analysis, the performance function is defined such that $y(\boldsymbol{x}) \le 0$ is considered failure. Thus, for the case of stress constraints, the following performance function is defined:

$$y(\boldsymbol{x}) := \sigma_{\text{limit}} - \sigma_A(\boldsymbol{x}) \tag{7}$$

where σ_A is the stress at location A.

A. SRS for the Torque-Arm Model

To show how the SRS is constructed and the PDF of the output is calculated, the three random variables, x_2, x_6, and x_8 that most significantly contribute to the stress performance are chosen. The coefficients of the polynomial chaos expansion are obtained using the performance values at collocation points. The collocation points are selected among the roots of the polynomial that is one order higher than the order of polynomial chaos expansion considered under restrictions of symmetry and closeness to the mean.[13]

In the torque-arm model, the PDF of the performance function is plotted in Fig. 2a for different orders of polynomials. There are 27 collocation points used for the second-order SRS and 125 points for

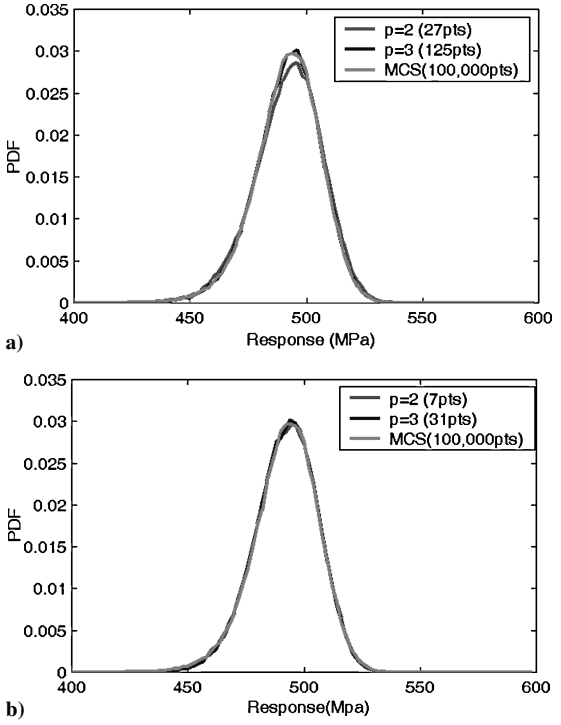

Fig. 2 PDF of the performance function y($\boldsymbol{x}$): a) only function values used with full collocations and b) function values and local sensitivities used with reduced collocations.

the third-order SRS. The accuracy and convergence of the proposed SRSs are compared with the PDF obtained using Monte Carlo simulation with 100,000 sampling points. The root-mean-square error of the second-order SRS is 5.7824×10^{-4} and the third-order SRS is 3.6012×10^{-4}. As expected, the error is reduced as the order of the polynomial is increased.

To reduce the required number of sampling points, local sensitivity information is now incorporated. In such a case, $n+1$ data are available (function value plus gradients of n random variables) at each sampling point. In the context of the case study, even if the number of unknown coefficients is not changed, the number of data that can be obtained from each sampling point is increased from one to four. Thus, theoretically, the number of sampling points can be reduced by a factor of four. In Fig. 2b, the PDF of the performance function is plotted for different orders of polynomials and that from the Monte Carlo simulation now considering local sensitivity information. It turns out that the SRS constructed using local sensitivity information can achieve the same level of accuracy as those constructed without sensitivity information with four times lower number of sampling points.

B. RBDO

The RBDO problem is formulated and solved for the torque-arm model using the third-order SRS. The design optimization problem is defined as minimize mass subject to

$$P(y_i(\boldsymbol{x}) \le 0) \le \Phi(-\beta_{t_i}), \qquad i = 1, \ldots, NC$$

$$\boldsymbol{d}^L \le \boldsymbol{d} \le \boldsymbol{d}^U \tag{8}$$

where $\boldsymbol{x} = [x_i]^T$, $i = 1, 2, \ldots, n$, denotes the vector of random variables, $\boldsymbol{d} = [d_i]^T = [\mu_i]^T$ represents the design variables chosen as the mean values of $\boldsymbol{x}$, β_t is the target reliability index, and Φ is the cumulative density function of SRV. The system performance criteria are described by the performance functions $y_j(\boldsymbol{x})$ such that the system fails if $y_j(\boldsymbol{x}) < 0$. Each $y_j(\boldsymbol{x})$ is characterized by its cumulative distribution function $F_y(0)$,

$$F_y(0) = P(y(\boldsymbol{x}) < 0) = \int_{y(\boldsymbol{x})<0} \cdots \int f_x(\boldsymbol{x})\, \mathrm{d}x_1 \cdots \mathrm{d}x_n \tag{9}$$

where $f_x(\boldsymbol{x})$ is the joint PDF of all random variables. During the optimization a $\beta_t = 3$ is used, which corresponds to 99.87% reliability. Because the maximum stress location can move, the probabilities of failure at four different locations are chosen as constraints in Eq. (8).

Because the probability integration domain is in general complex, many approximation methods [Monte Carlo simulation (MCS), first-order reliability method (FORM), or second-order reliability method (SORM)] are often used. In this Note, the PDF estimated using the proposed uncertainty propagation scheme is used for evaluating reliability constraints, hence, providing better approximations than the traditional linearization (FORM) at the current design and, thus, significantly improving the rate of convergence of RBDO.

Table 1 shows the properties of the random variables and the lower and upper bounds of their mean values (design parameters). In contrast to Sec. IV.A, in this model all eight random variables are subject of optimization.

Table 1 Definition of random design variables and their bounds

RV	d^L	d, Initial	d^U	d, Optimum	Standard deviation	Distribution type
x_1	−3.0	0	1.0	−0.7532	0.1	Normal
x_2	−0.5	0	1.0	−0.5000	0.1	Normal
x_3	−1.0	0	1.0	−0.1346	0.1	Normal
x_4	−2.7	0	1.0	−2.5443	0.1	Normal
x_5	−5.5	0	1.0	−0.8508	0.1	Normal
x_6	−0.5	0	2.0	1.9998	0.1	Normal
x_7	−1.0	0	7.0	0.8319	0.1	Normal
x_8	−0.5	0	0.0	0.0000	0.1	Normal

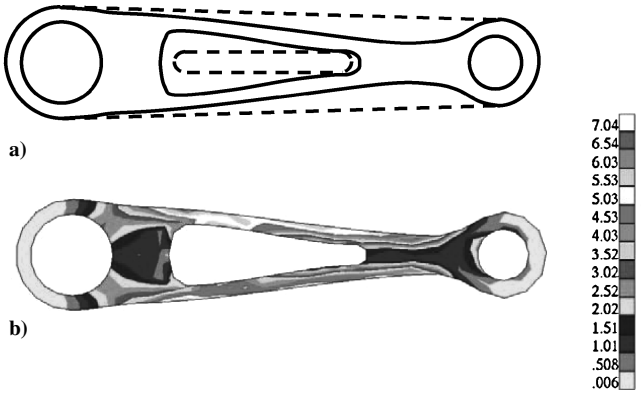

Fig. 3 Optimization results: a) geometry of the torque-arm model: - - -, initial and ——, optimum and b) maximum stress contour plot at optimum design.

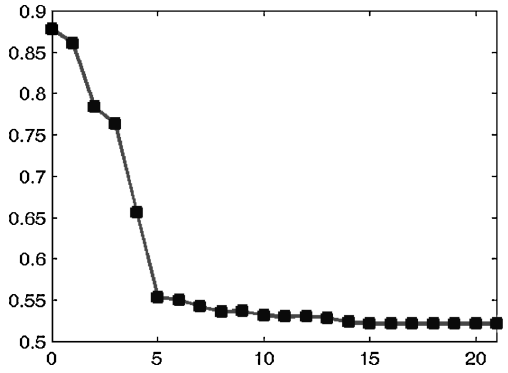

Fig. 4 Mass values for the torque-arm along the design process.

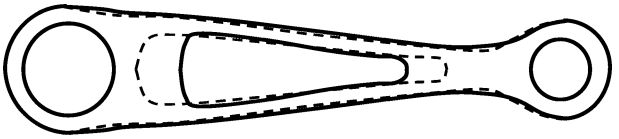

Fig. 5 Torque-arm problem results: - - -, deteministic and ——, reliability-based optimization.

The design optimization problem is solved using the sequential quadratic programming technique. The optimum values of the design variables are shown in the fifth column in Table 1. Figure 3 shows the optimum design and analysis results at the mean values. The major changes occur at design parameters d_4, d_5, and d_6. Even if the maximum stress constraint is set to 800 MPa, the optimum design converges to 704 MPa so that the variance of the input parameters can be accounted for. Figure 4 provides the optimization history of the cost function. As a result of the optimization process, the mass of the structure is reduced from 0.878 to 0.509 kg (a reduction of about 42%). Note that most of the reduction is achieved in the first five design cycles.

Figure 5 shows a comparison of the deterministic optimum design with that corresponding to RBDO. The dotted line represents the boundary curves of the deterministic optimum design, whereas the solid line represents the boundary curve of the reliability-based optimum design. The deterministic design has a larger inner slot size compared to the reliability-based optimization because the former does not account for the uncertainty in the design parameters and the corresponding variability in the performance function.

To see the impact of the accuracy of the uncertainty propagation procedure at the optimum design, a third-order SRS at optimum design is investigated (Fig. 6). The standard deviation is increased compared to the initial design. Table 2 shows the values of the reliability indices at the optimum design obtained from MCS, the proposed SRS approach, and the FORM. The proposed SRS approach

Table 2 Comparison of reliability indices at optimum design

Method	Reliability index	Error, %
MCS	3.0307	——
SRS	3.0115	0.633
FORM	2.9532	2.556

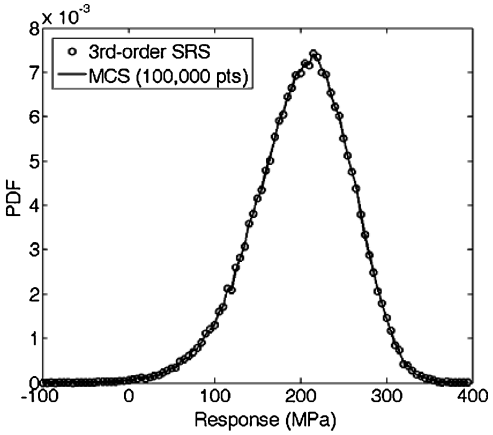

Fig. 6 PDF of the performance function at the optimum design for the torque-arm problem.

exhibits a lower error than the FORM and compares very well with the exact result, namely, 3.0, and that obtained using MCS, 0.6% error.

V. Conclusions

In this Note, we present an efficient RBDO framework based on polynomial chaos expansions (SRS) and local sensitivities. The polynomial chaos expansion, orthogonal with respect to the Gaussian measure, provides a convergent and robust uncertainty propagation scheme. The efficiency of the proposed SRS is improved by using local sensitivity information. The accuracy, efficiency, and convergence of the proposed approach for RBDO are demonstrated using a benchmark problem related to the RBBO of a structural part.

In general, as the nonlinearity of the problem increases, the errors using the traditional moment-based methods are expected to increase, whereas the proposed approach can still maintain its accuracy, although this may come at an additional computational expense.

References

[1]Enevoldsen, I., "Reliability-Based Optimization as an Information Tool," *Mechanics of Structures and Machines*, Vol. 22, No. 1, 1994, pp. 117–135.

[2]Lee, T. W., and Kwak, B. M., "A Reliability-Based Optimal Design Using Advanced First Order Second Moment Method," *Mechanics of Structures and Machines*, Vol. 15, No. 4, 1987, pp. 523–542.

[3]Tu, J., Choi, K. K., and Park, Y. H., "A New Study on Reliability-Based Design Optimization," *Journal of Mechanical Design*, Vol. 121, No. 4, 1999, pp. 557–564.

[4]Qu, X., and Haftka, R. T., "Reliability-Based Design Optimization Using Probability Sufficiency Factor," *Structural and Multidisciplinary Optimization*, Vol. 27, No. 5, 2004, pp. 314–325.

[5]Tatang, M. A., Pan, W. W., Prinn, R. G., and McRae, G. J., "An Efficient Method for Parametric Uncertainty Analysis of Numerical Geophysical Model," *Journal of Geophysical Research–Atmospheres*, Vol. 102, No. 8, 1997, pp. 21,925–21,932.

[6]Isukapalli, S. S., Roy, A., and Georgopoulos, P. G., "Stochastic Response Surface Methods (SRSM) for Uncertainty Propagation: Application to Environmental and Biological Systems," *Risk Analysis*, Vol. 18, No. 3, 1998, pp. 351–363.

[7]Anile, A. M., Spinella, S., and Rinaudo, S., "Stochastic Response Surface Method and Tolerance Analysis in Microelectronics," *International Journal for Computation and Mathematics in Electrical and Electronic Engineering*, Vol. 22, No. 2, 2003, pp. 314–327.

[8]Kim, Y. K., Hong, J.-P., and Hur, J., "Torque Characteristic Analysis Considering the Manufacturing Tolerance for Electric Machine by Stochastic Response Surface Method," *IEEE Transactions on Industry Applications*, Vol. 39, No. 3, 2003, pp. 713–719.

[9]Ghanem, R. G., and Spanos, P. D., *Stochastic Finite Elements: A Spectral Approach*, Springer-Verlag, New York, 1991.

[10]Isukapalli, S. S., Roy, A., and Georgopoulos, P. G., "Efficient Sensitivity/Uncertainty Analysis Using the Combined Stochastic Response Surface Method and Automated Differentiation: Application to Environmental and Biological Systems," *Risk Analysis*, Vol. 20, No. 5, 2000, pp. 591–602.

[11]Choi, K. K., and Kim, N. H., *Structural Sensitivity Analysis and Optimization: Vol. 1 Linear Systems*, Springer-Verlag, New York, 2004.

[12]Kim, N. H., Choi, K. K., and Botkin, M. E., "Numerical Method for Shape Optimization Using Meshfree Method," *Structural and Multidisciplinary Optimization*, Vol. 24, No. 6, 2003, pp. 418–429.

[13]Villadsen, J., and Michelsen, M. L., *Solution of Differential Equation Models by Polynomial Approximation*, Prentice–Hall, Englewood Cliffs, NJ, 1978.

S. Saigal
Associate Editor